Island sizes and capture zone areas in submonolayer deposition: Scaling and factorization of the joint probability distribution

J. W. Evans

Department of Mathematics and Ames Laboratory–USDOE, Iowa State University, Ames, Iowa 50011

M. C. Bartelt

Department of Chemistry and Materials Science, Lawrence Livermore National Laboratory, Livermore, California 94550

The joint probability distribution (JPD) for island sizes, s, and capture zone areas, A, provides extensive information on the distribution of islands formed during submonolayer deposition. For irreversible island formation via homogeneous nucleation, this JPD is shown to display scaling of the type $F(s/s_{av}, A/A_{av})$, where "av" denotes average values. The form of F reflects both a broad monomodal distribution of island sizes, and a significant spread of capture zone areas for each island size. A key ingredient determining this scaling behavior is the impact of each nucleation event on existing capture zone areas, which we quantify by kinetic Monte Carlo simulations. Combining this characterization of the spatial aspects of nucleation with a simplified but realistic factorization ansatz for the JPD, we provide a concise rate equation formulation for the variation of both the capture zone area and the island density with island size. This is achieved by analysis of the first two moments of the evolution equations for the JPD.

I. INTRODUCTION

A long-standing challenge in characterizing the early stages of epitaxial film growth (i.e., submonolayer deposition) has been to determine the analytic form of the size distribution of islands formed under conditions of homogeneous nucleation.[1] This challenge is non-trivial even in the simplest case of irreversible island formation. In the last decade, it has become clear that standard mean-field rate equations for densities, N_s, of islands of different sizes, s, fail to produce size distributions observed in simulation.[2,3] Analysis of these rate equations requires as input the "capture numbers," σ_s, which describe the propensity for islands of different sizes to capture diffusing adatoms. The σ_s are traditionally calculated in a self-consistent fashion from a diffusion equation analysis of the adatom density near islands.[3] However, this analysis of σ_s is based on a mean-field assumption that the typical environment of each island is independent of its size,[3,4] and we have recently shown that this assumption is fundamentally flawed.[5] Another perspective on adatom capture comes from the feature, noted long ago, that the capture numbers describing the growth rate of islands are directly related to the area of suitably constructed "capture zones" (CZs) surrounding the islands.[6] However, this observation did not in itself lead to a correct theoretical formulation of the island size distribution,[7] as one also needs a correct characterization of the relationship between CZ areas and island size.[5]

The key to an exact theory for the island size distribution is the recognition of two essential points. First, the island size distribution is controlled by the size dependence of the average capture number, σ_s, or average CZ area, A_s, for each island size, s. In fact, we have provided an exact integral formula relating these two quantities.[5] Second, this dependence of σ_s or A_s on s is qualitatively distinct from

mean-field predictions.[5] This is due to the feature that larger islands have on average substantially larger CZs. Thus, in contrast to the above mean-field picture, there is a subtle correlation between the size and separation of islands. This size-separation correlation is distinct from the well-known spatial correlation of island positions associated with depletion of the population of nearby islands.[4] Furthermore, the size-separation correlation is not embodied in the previous recognition of an obvious correlation between capture numbers and CZ areas.

It thus remains to provide an appropriate theory for the non-mean-field dependence of the σ_s or A_s, versus island size, s. Two approaches have been taken to address this challenge. Evans and Bartelt (EB) previously developed rate equations, which directly describe the evolution of the average CZ areas, A_s,[8,9] and which qualitatively recovered non-mean-field behavior. Mulheran and Robbie (MR)[10] developed rate equations for the joint probability distribution (JPD), $N_{s,A}$, for island sizes, s, and capture zone areas, A. This novel approach by MR provided a particularly natural (but somewhat complex) framework to analyze non-mean-field behavior, and also successfully recovered the observed behavior for average capture numbers and size distributions. Amar, Popescu, and Family (APF)[11,12] also utilized and solved a simplified form of the JPD equations to recover non-mean-field behavior of the key quantities. However, as we discuss in detail below, APFs idealized treatment of nucleation leads to a negligible spread in capture zone areas for each island size, in contrast to the physically observed behavior.

The existence of scaling of the JPD is a central feature of submonolayer island formation. This property of course incorporates the familiar scaling of the island size distribution. However, it further implies a "broad" spread of island sizes for each CZ area, and a "broad" spread of CZ areas for each island size. For example, the latter specifically means that for

each island size, the width of the CZ area distribution scales with the mean CZ area. These features are actually apparent in experimental data,[13] and are also reflected in previous theoretical analyses.[9,10] However, these previous studies lack the following ingredients, which are provided here: (i) precise simulation results showing scaling of the JPD; (ii) tailored simulation studies characterizing key spatial aspects of the nucleation process; and (iii) a concise theoretical formulation of scaling which incorporates a correct description of nucleation, and yet provides simple equation(s) which can be used to both predict and assess key properties of quantities such as the mean CZ area versus island size.

In Sec. II, we describe the point-island model for irreversible island formation, which is analyzed in this paper, as well as our algorithms for its simulation and analysis. Then, in Sec. III, we describe the scaling form of the JPD and associated reduced quantities, together with an approximate but realistic factorization ansatz for the JPD. We also present simulation results to support these ideas. Next, in Sec. IV, we provide a detailed characterization of the island nucleation process, and provide simulation results to quantify behavior. This characterization is crucial as nucleation behavior controls the detailed scaling form of the JPD. In Sec. V, we analyze the first two moments of the evolution equations for the JPD,[9] which yield simpler equations directly for the island densities, N_s, and average CZ areas, A_s. We present the scaling form of these moment equations in Sec. VI. The equation for A_s incorporates key information on nucleation, and is reduced to a concise form using the JPD factorization ansatz. Numerical results for the solution of this equation are presented in Sec. VII, and comparison is made with relevant simulation results. Finally, in Sec. VIII, we provide our conclusions, and also comment on differences in the behavior of key scaling functions for various island geometries.

II. MODEL PRESCRIPTION, SIMULATION, AND ANALYSIS

We shall consider in this paper only the simplest case of irreversible island formation during submonolayer deposition on a single-crystal surface represented by a square lattice of adsorption sites: adatoms are deposited randomly at a rate of F per adsorption site, they hop between adjacent sites at rate h (per direction), irreversibly nucleate new islands upon meeting, and irreversibly incorporate with existing islands upon aggregation. Atoms landing "directly" on-top of an island are regarded as instantaneously incorporated at the island edge. One canonical class of models incorporates compact shapes for individual islands associated with efficient (or instantaneous) restructuring upon aggregation or direct on-top deposition.[14] Such models are computationally efficient, but also effective in realistically modeling numerous specific systems. To describe behavior at very low coverages (where islands cover only a small fraction of the surface), and to elucidate fundamental issues regarding the scaling of island densities and size distributions, it is convenient to consider even simpler "point-island" models.[2] In these models, islands occupy only a single site, but carry a label indicating their size. The following formulation applies

to both compact and point island cases, but we will present simulation results only for point islands. Below, we shall use the surface lattice constant, a, as the unit of length (and, correspondingly, the adsorption site as the unit of area). Thus, adatom densities (N_1) and island densities (N_s) are measured per adsorption site, the adatom diffusion coefficient $D = a^2 h$ will correspond to the hop rate h per direction for a square lattice, etc. The coverage, $\theta = Ft$, is given in monolayers (ML), where t is the duration time of deposition.

A central concept in this paper is that of "capture zones" (CZs), which were briefly mentioned above. The underlying idea is that typically atoms deposited nearby an island within its CZ will aggregate with that island. Thus, the CZ area should measure the aggregation rate or capture number for that island, and thus its growth rate. Indeed, it is possible to construct CZs, based on the solution of an appropriate diffusion equation for deposited atoms, so that this relationship is exact. The construction of such "diffusion cells" (DCs) is described in detail elsewhere.[13] Indeed, the analytic theory developed in this paper is based on the assumption that the CZs are constructed as DCs, so that CZ areas exactly describe capture rates. This theory will also require a detailed characterization of the distribution of CZ areas. Furthermore, it will be necessary to monitor a number of quantities associated with just-nucleated islands and their CZs, which relate to how nucleation impacts on existing CZs (see below). However, construction of "exact" CZs is nontrivial, and computationally expensive. Thus, to facilitate acquisition of precise statistics for the JPD, and related quantities, we will construct CZs approximately, based on geometric tessellations of the island distribution. The simplest possibility is to use Voronoi cells (VCs), which are based on the distance from the island centers.[5–7] A more realistic alternative for compact islands is to use "edge cells" (ECs) which are based on the distance to island edges.[7,13] Of course, VCs and ECs coincide for point islands. See Refs. 5, 7, and 13 for a more detailed discussion.

Next we provide some brief comments on our algorithms for simulation and analysis of the point-island model on an $L \times L$ square lattice with periodic boundary conditions. Typically, our simulations will be performed in the "scaling regime" (see below) of large $h/F = 10^7 - 10^9$. Because of this large difference in rates, efficient simulation requires a Bortz-type algorithm, where one keeps a list of the positions of all hopping adatoms. With probabilities proportional to total rates, one randomly chooses between deposition (total rate $L^2 F$), and hopping (total rate $4h$ *times* the number of hopping adatoms). For the former, one randomly chooses a site. For the latter, one randomly chooses a hopping adatom from the list, which is updated after each hopping, deposition or aggregation event. As indicated above, in the point-island model, one must maintain a counter for each island which tracks its size, and which is continually updated for each aggregation event. In this way, one can readily extract information on island size distributions. We will also determine some information on capture numbers (and thus on "exact" CZ areas) by monitoring the rate of adatoms aggregating with individual islands using procedures that are described in Ref. 5. As indicated above, for more detailed and compre-

TABLE I. Key quantities and their scaling functions. See the text for detailed definitions.

Quantity	Notation	Scaling function
Joint probability distribution	$N_{s,A}$	$F(x,\alpha)$
Island size distribution	$N_s = \Sigma_A N_{s,A}$	$f(x)$
CZ area distribution	$N_A = \Sigma_s N_{s,A}$	$g(\alpha)$
Nucleated CZ overlap probability	$P_{s,A}$	$q(\alpha)$
Nucleated CZ overlap subarea	$A_{\text{subnuc}}(s,A)$	$a_{\text{subnuc}}(\alpha)$
Mean CZ area for islands of size s	A_s	$a(x)$

hensive analysis of the JPD and related quantities, we will approximate CZs by VCs which are constructed for each island to correspond to the set of sites closer to that island than to others. (Sites equidistant from two or more islands are somewhat arbitrarily assigned to one island, but the fraction of such sites becomes insignificant in the scaling limit.)

III. THE JOINT PROBABILITY DISTRIBUTION (JPD): SCALING AND FACTORIZATION

We now list the key quantities of interest in our analysis (see Table I), as well as their proposed scaling forms. As in Sec. I, we let $N_{s,A}$ denote the density of islands with size s (measured in adatoms) and CZ area A (measured in sites). Also CZ areas will be defined here to include the area of the island contained within them (although this area is not significant for point islands). Then, the density, N_s, of islands of size s satisfies $N_s = \Sigma_A N_{s,A}$, and the average island density satisfies $N_{\text{av}} = \Sigma_{s>1} N_s$. The average CZ area for islands

of size s satisfies $A_s = \Sigma_A A N_{s,A}/N_s$. Since $\Sigma_{s>1}\Sigma_A A N_{s,A} = 1$, it follows that $A_{\text{av}} = \Sigma_{s>1} A_s N_s/N_{\text{av}} = 1/N_{\text{av}}$. The coverage satisfies $\theta = \Sigma_s s N_s$, and the average island size satisfies $s_{\text{av}} = \Sigma_{s>1} s N_s/N_{\text{av}} = (\theta - N_1)/N_{\text{av}}$. In the scaling regime of large h/F or large $s_{\text{av}} \approx \theta/N_{\text{av}}$, it is natural to look for suitable scaling forms of these quantities.[2,5,8–10] Specifically, one introduces continuous scaled variables $x = s/s_{\text{av}} \geq 0$ and $\alpha = A/A_{\text{av}} \geq 0$, and writes

$$N_{s,A} \approx N_{\text{av}}(s_{\text{av}}A_{\text{av}})^{-1}F(x,\alpha), \quad N_s \approx N_{\text{av}}(s_{\text{av}})^{-1}f(x),$$

$$A_s \approx A_{\text{av}}a(x). \tag{1}$$

One has the normalization conditions $\int dx \int d\alpha\, F(x,\alpha)x^i\alpha^j = 1$, for i or $j = 0$ or 1. It follows that $f(x) = \int d\alpha\, F(x,\alpha)$ and $f(x)a(x) = \int d\alpha\, F(x,\alpha)\alpha$, so that $\int dx\, f(x)x^i = 1$, for $i = 0$ or 1, and $\int dx\, a(x)f(x) = 1$. Here and in the following, integrals over these variables always range from 0 to ∞. It is also instructive to characterize the CZ area distribution $N_A = \Sigma_s N_{s,A} \approx N_{\text{av}}(A_{\text{av}})^{-1}g(\alpha)$, where $g(\alpha) = \int dx\, F(x,\alpha)$.

Next, we present a comprehensive set of simulation results for these quantities for the point-island model. Again, we note that CZs are typically approximated as VCs in this analysis. First, in Fig. 1, we show a typical distribution of islands (labeled by their size) and the associated VCs for $h/F = 10^{10}$ at 0.1 ML in a 500×500 system. Note that small islands can have large CZs or VCs, since we shall see that the average CZ or VC area for just nucleated islands is only slightly below the average, and there is a large variation in areas for each size. In Fig. 2, we present both 3D and contour plot representations of the behavior of the JPD $F(x,\alpha)$ for $h/F = 10^7$ at 0.1 ML. Figure 3 demonstrates scaling of the
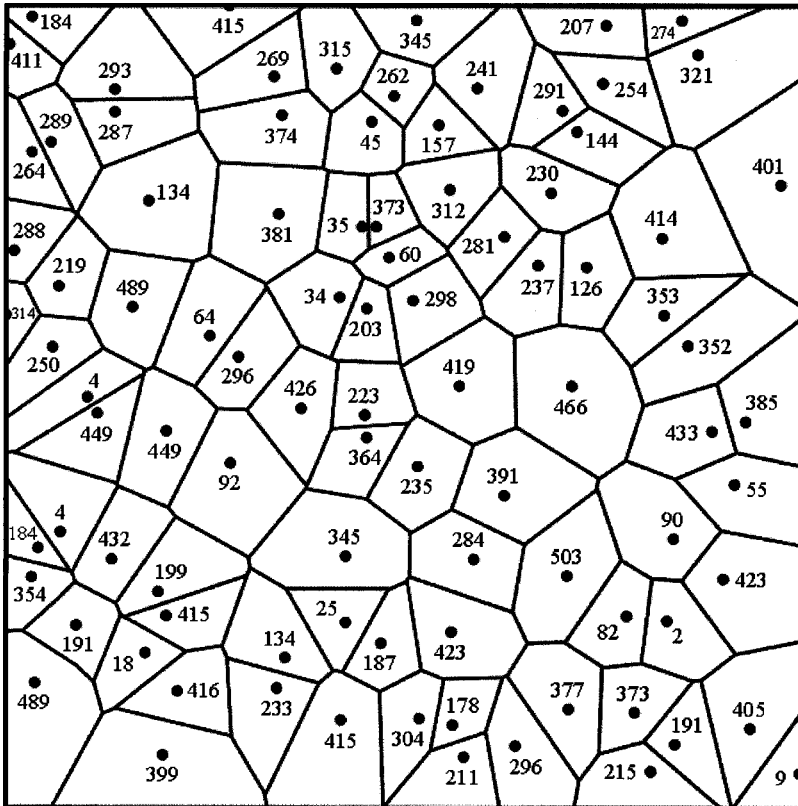

FIG. 1. Simulated island configuration, sizes, and associated VCs for point islands with $h/F = 10^{10}$ at 0.1 ML on a 500×500 site lattice.
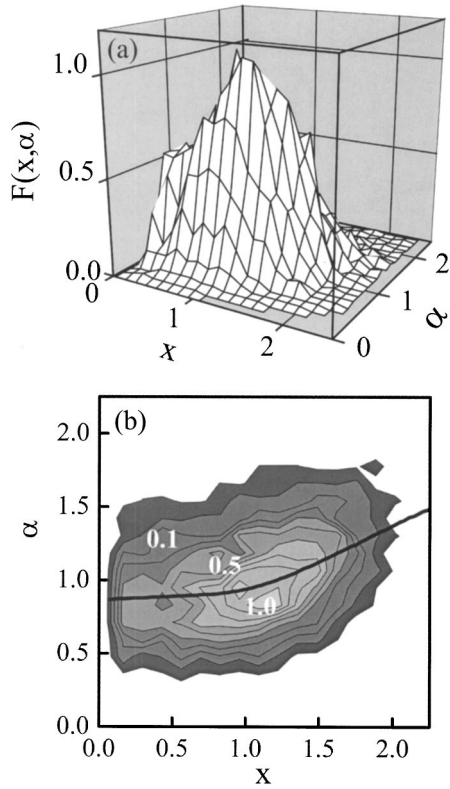
FIG. 2. (a) 3D plot, and (b) contour plot of $F(x,\alpha)$ $=(s_{av}/N_{av}^2)N_{s,A}$ versus $x=s/s_{av}$ and $\alpha=A/A_{av}$. The curve α $=a(x)$ (i.e., the scaled mean CZ area for each scaled island size) is superimposed on the contour plot. Simulation data is for point islands with $h/F=10^7$, 0.1 ML: $s_{av}=30.7$ and $A_{av}=307$.

island size distribution which determines $f(x)$, and of the CZ area distribution which determines $g(\alpha)$. Figure 4(a) demonstrates scaling of the mean capture number for islands of a specific size versus island size. This quantity determines the scaling behavior of the "exact" CZ areas, and thus of the exact $a(x)$. For contrast, in Fig. 4(b), we show the scaling of the mean VC area as a function of island size. The corresponding scaling function, $a_{VC}(x)$, satisfies $a(x)$ $\approx 0.7a_{VC}(x)+0.3$,[5] illustrating the general similarity (but also subtle differences) between exact CZs and VCs. One transparent feature of the point-island model is that the mean-field form of the mean CZ area satisfies $A_s=A_{av}$ or
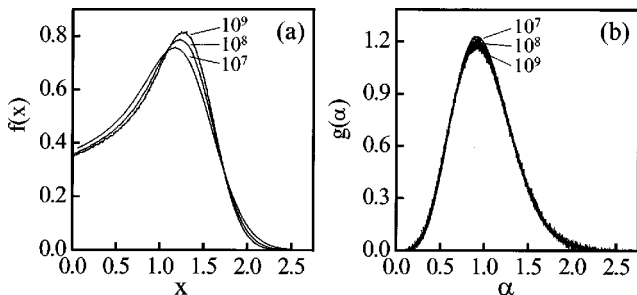

FIG. 3. (a) $f(x)=(s_{av}/N_{av})N_s$ versus $x=s/s_{av}$; (b) $g(\alpha)$ $=(A_{av}/N_{av})N_A$ versus $\alpha=A/A_{av}$. Simulation data is for point islands with $h/F=10^7-10^9$ at 0.1 ML.
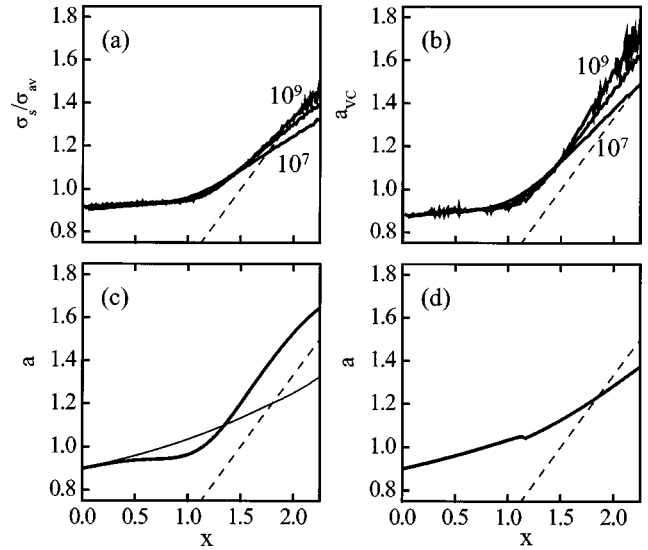

FIG. 4. (a) Exact $a(x)=\sigma_s/\sigma_{av}$ versus x; (b) $a_{VC}(x)$ versus x (for VCs). Simulation data is for point islands with h/F $=10^7-10^9$ at 0.1 ML. (c) Numerical solution of Eq. (16) for $a(x)$ versus x with simulation data for $f(x)$ as input to the last term on the RHS, and choosing $c\mu=0.675$ (thick curve). The result of ignoring the last term on the RHS of (16) is also shown (thin curve). (d) Numerical solution of Eq. (17) for $a(x)$ versus x, and choosing $c\mu=0.6$, and where we jump over the singular point at $x=x_s$ ≈ 1.03. In plots (a)–(d), the dashed line shows $a=z\cdot x$ with z $=2/3$.

$a_{mf}(x)=1$. Thus, the variation of $a(x)$ versus x apparent in Fig. 4 [as well as that of $a_{VC}(x)$] clearly contrasts mean-field behavior, and is critical in determining the shape of the island size distribution (see Sec. VI and Ref. 5).

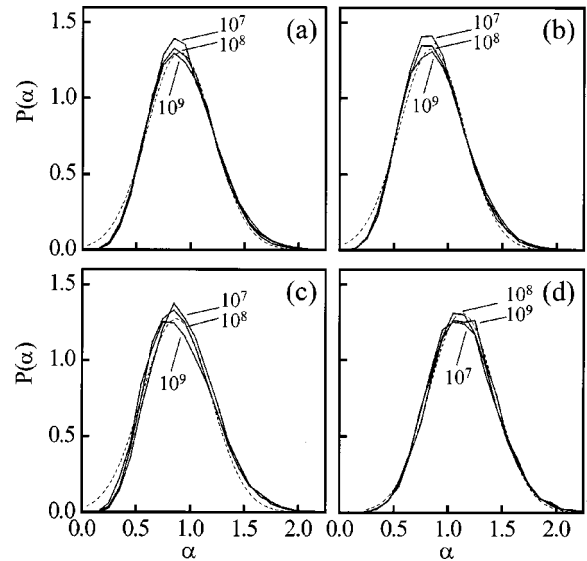Finally, we return to a more detailed characterization of

FIG. 5. Scaled area distributions for VCs for (a) just nucleated islands, (b) dimers, (c) islands of size $s=s_{av}$, and (d) islands of size $s=1.5s_{av}$. Simulation data is for point islands with h/F $=10^7-10^9$ at 0.1 ML. The dashed lines are Gaussian fits. See Table II for details.
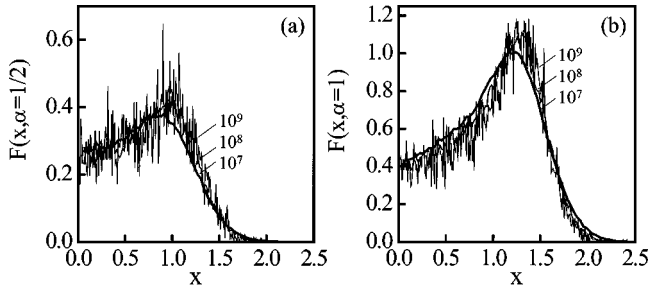
FIG. 6. Scaled size distributions for islands of fixed CZ area, (a) $A = 0.5A_{av}$ (average island size $\approx 0.7s_{av}$) and (b) $A = A_{av}$ (average island size $\approx s_{av}$). Simulation data is for point islands with $h/F = 10^7 - 10^9$ at 0.1 ML. The Poisson distributions used by APF (Refs. 11 and 12) to describe size distributions for $A > A_2$ are much narrower.

the JPD. In Fig. 5, we present 2D plots for the scaling of the VC area distribution for just nucleated islands, for dimers ($s = 2$), for islands of size $s = s_{av}$, and of size $s = 1.5s_{av}$. The latter three distributions determine $F(0+, \alpha)$, $F(1, \alpha)$, and $F(1.5, \alpha)$ versus α, respectively. In Fig. 6, we present 2D plots of the island size distribution for fixed VC area $A = 0.5A_{av}$ and $A = A_{av}$. These two distributions determine $F(x, 0.5)$ and $F(x, 1)$ versus x, respectively. Some of the properties of these distributions are summarized in Table II. One significant feature noted previously,[9] and used in our subsequent analysis, is that $v(x) = \int d\alpha [\alpha - a(x)]^2 F(x, \alpha)$ is roughly independent of x. This quantity denotes the variance of the scaled VC area distribution for islands of a specific scaled size x.

As noted above, the treatment of APF produces a ''narrow'' Poisson distribution of island sizes for each CZ area, and an associated ''singular'' delta-function scaling form for $F(x, \alpha) = \delta(\alpha - a(x))f(x)$ in the scaling limit.[15] In contrast, Fig. 5 shows the actual broad scaling form of $F(x, \alpha)$ versus α, for each fixed x, and Fig. 6(a) shows that $F(x, \alpha)$ does not vanish for $\alpha < \min_x a(x) = a(0)$. In fact, it is natural to invoke a factorization ansatz for $F(x, \alpha)$. Specifically, we shall assume that the shape of the normalized distribution of scaled CZ areas for each scaled island size, x, is roughly independent of x. This hypothesis is supported by the extensive data presented in Fig. 7. Thus, the distribution of scaled CZ areas
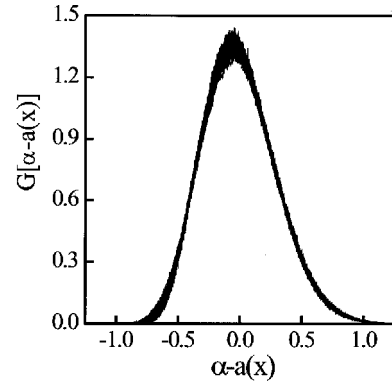

FIG. 7. Detailed test of the factorization hypothesis for the JPD. Collapsed plots for the shape of the CZ area distribution, $G = F(x, \alpha)/f(x)$, versus $\alpha - a(x)$, using data for all $x \lesssim 1.5$. The distribution, G, becomes somewhat broader and less skewed for higher $x \approx 2$. However, F has little weight in this x range, so this slight deviation from factorization is not significant. Simulation data are for point islands with $h/F = 10^7$, 0.1 ML.

(for each x) merely shifts its mean to $a(x)$, and adjusts its normalization to $f(x)$, with varying x. This implies the relation

$$F(x, \alpha) = G[\alpha - a(x)]f(x), \qquad (2)$$

where G gives the shape of the CZ area distribution. This G satisfies $\int d\gamma \, G(\gamma) = 1$, $\int d\gamma \, G(\gamma)\gamma = 0$, and $\int d\gamma \, G(\gamma)\gamma^2 = v$. This ansatz (2) is consistent with roughly constant $v(x) \approx v$ mentioned above. In fact, it is reasonable to adopt a Gaussian approximation $G(\gamma) = (2\pi)^{-1/2} v^{-1/2} \exp[-\gamma^2/(2v)]$, although simulation results reveal some skewness in the CZ area distributions. See Fig. 7 and Table II.

IV. REALISTIC CHARACTERIZATION OF THE NUCLEATION PROCESS

The importance of a realistic description of island nucleation in formulating theories for capture zone evolution is discussed in Ref. 9. Here, we summarize the basic features of irreversible island formation as determined by a traditional rate equation analysis. In the initial stage of deposition, there is a *transient* regime where the adatom concentration in-

TABLE II. Statistical properties of the area distributions for VCs of point islands of a fixed size. Results shown correspond to $h/F = 10^7$ ($s_{av} = 30.70$, $A_{av} = 307.0$), 10^8 ($s_{av} = 61.27$, $A_{av} = 612.7$), and 10^9 ($s_{av} = 124.39$, $A_{av} = 1243.9$), and $\theta = 0.1$ ML. Areas and standard deviations are in units of surface sites. The skewness is dimensionless.

	Average area			Standard deviation			Skewness		
Island size	10^7	10^8	10^9	10^7	10^8	10^9	10^7	10^8	10^9
Just-nucleated Islands ($s = 2$)	284.7	572.7	1165.0	88.6	182.8	381.3	0.40	0.42	0.42
All dimers ($s = 2$)	268.3	537.5	1098.1	87.7	179.2	374.2	0.45	0.45	0.45
$s = s_{av}$	289.7	567.9	1140.1	91.6	186.0	390.3	0.44	0.49	0.48
$s = 1.5 s_{av}$	347.1	693.5	1425.5	94.4	185.9	376.7	0.29	0.29	0.23

creases linearly with time. Subsequently, a *steady-state* regime develops, wherein gain of adatoms due to deposition is roughly balanced by the loss due to aggregation with existing islands. Specifically, for small θ, one has

$$d/dt\,N_1 \sim F - \sigma_{av} h N_1 N_{av} \quad \text{and} \quad d/dt\,N_{av} \sim \sigma_1 h (N_1)^2, \tag{3}$$

so it follows that

$$N_1 \sim \theta \quad \text{and} \quad N_{av} \sim (h/F)\theta^3, \tag{4a}$$

for the transient regime where $\theta \ll \theta^* \sim (h/F)^{-1/2}$, and

$$N_1 \sim (h/F)^{-2/3}\theta^{-1/3} \quad \text{and} \quad N_{av} \sim (h/F)^{-1/3}\theta^{1/3}, \tag{4b}$$

for the steady-state regime where $\theta \gg \theta^* \sim (h/F)^{-1/2}$. However, the steady-state θ dependence is significantly modified for compact islands, even for small $\theta \ll 1$. At the crossover between transient and steady-state regimes, $N_{av}(\theta \sim \theta^*) \sim (h/F)^{-1/2}$ is well below the subsequent steady-state value of $N_{av} \sim (h/F)^{-1/3}$. Thus, most nucleation occurs in the steady-state regime for $\theta^* \ll \theta \ll O(1)$. This persistence of nucleation is fundamental to the detailed development of these CZ distributions, and in fact underlies the existence of nontrivial scaling solutions.[5,9] Clearly, continued nucleation will impact existing CZs, and produce a nontrivial distribution of CZ areas for islands of each size. Consequently, our following analysis is focused on the steady-state regime.

For an appropriate treatment of the evolution of the CZ areas and of the JPD, a more detailed characterization of the spatial aspects of nucleation is critical. As noted previously,[9,16] most nucleation (in the steady-state regime) must occur near the boundaries of CZs where the adatom density (and thus the nucleation rate) is relatively high. This feature will be incorporated into our formulation below. It is instructive to contrast this picture with other approaches. MR[10] adopt a fragmentation picture, wherein each new nucleation event fragments an existing CZ into two parts. Although somewhat unrealistic, this picture is able to successfully incorporate important effects of nucleation on the evolution of the CZ distribution. The rather different APF formulation[11,12] introduces a new CZ associated with each nucleation event (or just-nucleated island), which has an area simply related to the average CZ area at the time of nucleation. However, this procedure does not account for the impact of nucleation events on areas of existing CZs other than by global rescaling to maintain a constant total area of CZs. As a consequence, it produces an artificially narrow (Poisson) distribution of island sizes for each area A, and thus an artificially narrow distribution of CZ areas for each size.

Our analysis of evolution of the JPD in Sec. V will involve two key quantities characterizing nucleation. See Table I. First, let $P_{s,A}$ denote the probability that a nucleation event "impacts" a CZ of area A belonging to an island of size s. This means that the CZ of the just-nucleated island overlaps (and thus reduces) the CZ of this existing island of size s. See Appendix A for more details. Second, in the event of such overlap, let $A_{subnuc}(s,A)$ denote the average area of the portion or subset of the CZ of the just-nucleated island which overlaps the existing CZ of area A. See the schematic in Fig.
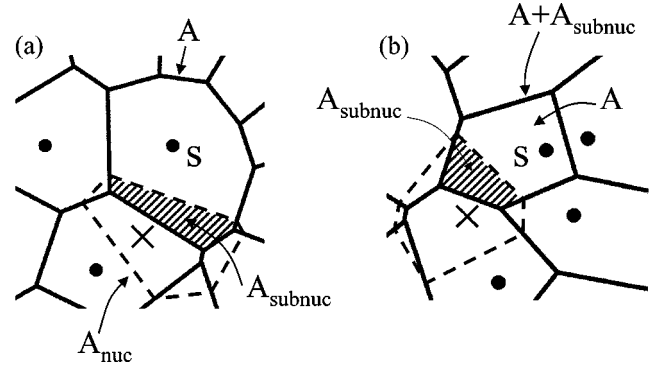

FIG. 8. Nucleation events ($\times$) contributing to (a) $P_{s,A}$, and more specifically to $P_{s,A}(A_{subnuc})$; (b) $P_{s,A}^+$, and more specifically to $P_{s,A+Asubnuc}(A_{subnuc})$. See the text and Appendix A. CZ boundaries of islands existing before the nucleation event are indicated by thick solid lines. The CZ boundary of the just-nucleated island is indicated by dashed lines.

8.[17] Furthermore, we let M_0 denote the average number of existing CZs overlapped by the CZ of a just-nucleated island, and let $A_{avsubnuc}$ denote the average area of the individual portions or subsets of the CZs of just-nucleated islands overlapping each existing CZ. Then, one has the normalization conditions

$$\Sigma_s \Sigma_A P_{s,A} = M_0 \quad \text{and} \quad \Sigma_s \Sigma_A A_{subnuc}(s,A)P_{s,A} = A_{avsubnuc}M_0. \tag{5}$$

Our simulation analyses for point islands indicates that $M_0 \approx 5.5$ for $h/F = 10^7$ at $\theta = 0.1$ ML (increasingly slowly with h/F, to 5.6 for $h/F = 10^8$ and 5.7 for $h/F = 10^9$).

For these quantities, we assume the natural scaling forms

$$P_{s,A} \approx (N_{s,A}/N_{av})q(\alpha)$$

and $\qquad\qquad\qquad\qquad\qquad\qquad\qquad$ (6)

$$A_{subnuc}(s,A) \approx A_{av}a_{subnuc}(\alpha),$$

and write $A_{avsubnuc} = A_{av}a_{avsubnuc}$. Here, we have neglected any x dependence of q and a_{subnuc} based on the idea that the probability and nature of the impact of nucleation on existing CZs should depend primarily on their area A rather than on the size s of the associated island (cf. Refs. 10–12). This is certainly the case for point islands. One also has the normalization constraints that

$$\int dx \int d\alpha\, q(\alpha)F(x,\alpha) = M_0$$

and $\qquad\qquad\qquad\qquad\qquad\qquad\qquad$ (7)

$$\int dx \int d\alpha\, a_{subnuc}(\alpha)q(\alpha)F(x,\alpha) = a_{avsubnuc}M_0,$$

which can be rewritten as $\int d\alpha\, q(\alpha)g(\alpha) = M_0$ and $\int d\alpha\, a_{subnuc}(\alpha)q(\alpha)g(\alpha) = a_{avsubnuc}M_0$.

Next, we describe in more detail the expected behavior of these key quantities, and present simulation results for point islands to confirm these speculations. It is easiest to antici-
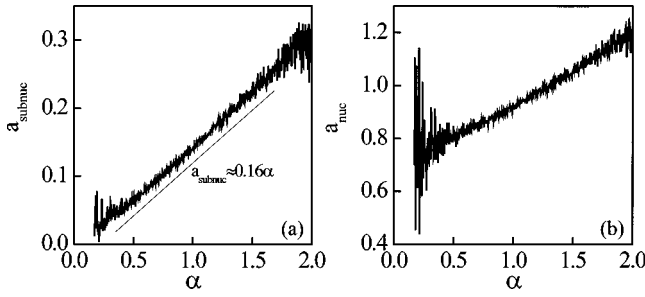
FIG. 9. (a) a_{subnuc} versus α; (b) a_{nuc} versus α. Simulation data for point islands with $h/F = 10^7$, 0.1 ML. The slope, μ, of a linear fit $a_{subnuc} \approx \mu \cdot \alpha$ is also indicated with $\mu \approx 0.16$.

FIG. 10. $q(\alpha)$ versus α. Simulation data for point islands with $h/F = 10^7$, (gray line) and $h/F = 10^8$ (black line) at 0.1 ML. The data collapse confirms scaling of this quantity, which is necessary for scaling of the JPD. Further details of its behavior will be discussed in a separate publication.

pate the behavior of A_{subnuc} or a_{subnuc} based on simple geometric considerations. The CZ of the just nucleated island will overlap on average M_0 existing CZ areas, and the extent of overlap should be *proportional* to the areas of the individual CZs. (Another perspective leading to this conclusion is that nucleation occurs primarily near the boundaries of existing CZs, and the CZ of the just nucleated island will extend roughly half way to the neighboring islands covering a fixed fraction of the existing CZs.) Thus, one concludes that $A_{subnuc}(s,A) \approx \mu \cdot A$, or equivalently $a_{subnuc}(\alpha) \approx \mu \cdot \alpha$, where we expect that $\mu \approx a_{avsubnuc}$ [assuming that $\int d\alpha \, \alpha q(\alpha) g(\alpha) \approx M_0$]. To estimate μ, note that $A_{avnuc} = A_{avsubnuc} M_0$ gives the average (total) area the CZs of just-nucleated islands, and set $A_{avnuc} = A_{av} a_{avnuc}$ (see Appendix A). Previous simulations for point islands showed that $a_{avnuc} \approx 0.97$,[5,9] so that $\mu \approx a_{avsubnuc} = a_{avnuc}/M_0 = 0.97/M_0 \approx 0.18$. Simulation data for point islands shown in Fig. 9 indeed indicates that $a_{subnuc}(\alpha) \approx \mu \cdot \alpha$, with $\mu \approx 0.16$ (for $h/F = 10^7$ and $\theta = 0.1$ ML).

Much more difficult is anticipation of the behavior of $P_{s,A}$ or, equivalently, of $q(\alpha)$. It is perhaps useful to start by determining the probability that nucleation occurs within a CZ of area A for which the island is in the center. In Appendix B, we analyze the steady-state solution of the appropriate diffusion equation for a circularly symmetric geometry, with zero adatom density at the island edge, and a zero flux boundary condition on the CZ boundary. Assuming that the nucleation rate within a CZ of area A scales like $P_{s,A}$, and neglecting logarithmic corrections, one concludes that $q(\alpha) \sim \alpha^n$ with $n = 3$ [cf. the MR form where $n = 4$ (Ref. 10)]. Certainly, our analysis is too simplistic. The exact $P_{s,A}$ incorporates contributions from nucleation events occurring not only within the cell of area A, but also in a neighboring cell of generally different size. However, this should not in itself greatly affect the above analysis. Even though adjacent CZs may have different sizes, the CZ boundaries near where most nucleation occurs are roughly midway between the edges of the island of interest and its neighbors (and exactly midway for ECs, or for VCs in the case of point islands).

However, some important features are certainly absent from the above analysis of nucleation. One of these is that CZs may be elongated (and still have the island in the center), a feature which seems more common for small CZs. Then, the CZ "radius," R, will vary significantly about its average value of $R_{av} = (A/\pi)^{1/2}$. This will have the effect of
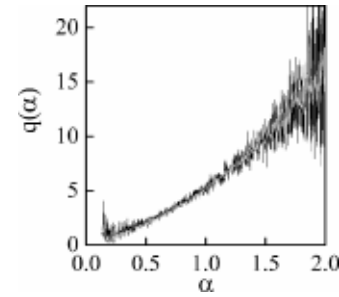
increasing the nucleation rate. Thus, $q(\alpha)$ will be enhanced for small α relative to our above analysis, perhaps replacing $n = 3$ by a lower effective exponent. Another feature which is an automatic consequence of adjacent CZs having different sizes is that the islands are typically not centered, so again R varies significantly about R_{av}. This feature likely occurs for all CZ sizes.

In Fig. 10, we show simulation results for point islands for $q(\alpha)$ versus α. These may be fit by a form, $q(\alpha) \approx c \cdot \alpha^{n_{eff}}$, where $n_{eff} \approx 2$ for small α, decreasing to $n_{eff} \approx 1.2$ for $\alpha \approx 1.5$, which can be approximated by $n_{eff} \approx (4+\alpha)/(2+\alpha)$. Our simulation data also confirms scaling of $q(\alpha)$ for different h/F. A more detailed analysis of this key quantity which characterizes nucleation (and of other related quantities), will be presented in a separate study.

We emphasize that analysis in Sec. V and Sec. VI of JPD equations, which incorporates the above type of realistic description of nucleation (and, specifically, the scaling forms for A_{subnuc} and $P_{s,A}$), does not just assume a scaling form for the JPD solutions (cf. Ref. 12). Rather, this analysis actually shows that this scaling form is consistent with the structure of the JPD equations. See also Refs. 9 and 10.

V. RATE EQUATIONS FOR THE JPD: MOMENT ANALYSIS

Development of evolution equations for the JPD, $N_{s,A}$, requires consideration of both island nucleation and growth. To simplify our analysis of island growth, we shall also assume that capture zones for each island are constructed as DC's so that their areas exactly describe the capture numbers or growth rates of the islands contained therein.[13] Specifically, this means that the rate of growth, r_{agg}, of a specific island with capture number σ due to capture or aggregation of diffusing adatoms equals the rate at which deposited atoms land within its CZ area of A (but not on top of the island). Thus, one has $r_{agg} = h\sigma N_1 = FA^f$, where for compact islands $A^f = A - s$ is the free area of the CZ not covered by the island. Growth of the island due to direct on-top deposition occurs at rate $r_{dep} = Fs$, so the total growth rate satisfies $r_{tot} = r_{agg} + r_{dep} = FA$. Obvious modification of r_{agg} and r_{dep} is required for point islands, but one obtains the same result for $r_{tot} = FA$ (for exact CZs).

To characterize the effect of island nucleation, we utilize $P_{s,A}$ introduced in Sec. IV which gives the probability that a nucleation event "impacts" the CZ of area A of an island of size s. We also utilize $P_{s,A}^+$ which denotes the probability that nucleation impacts the CZ of an island of size s so as produce a CZ of area A for that island, i.e., the existing CZ is reduced from some larger area to A. See Fig. 8. It then follows that $\Sigma_A P_{s,A} = \Sigma_A P_{s,A}^+ = P_s$ is the probability that nucleation impacts the CZ of some island of size s.[18] See also Appendix A. Note that $\Sigma_s P_s = M_0$ equals the average number of existing CZs overlapped by the CZ of a just nucleated island (cf. Sec. IV).

Thus, finally, we have the basic JPD evolution equations

$$d/dt\, N_{s,A} = FAN_{s-1,A} - FAN_{s,A} + P_{s,A}^+ d/dt\, N_{av}$$
$$- P_{s,A}\, d/dt\, N_{av}, \tag{8}$$

for $s > 2$. The first two terms describe the effects of island growth, and the latter two the effects of nucleation. We now perform a moment analysis of (8) by first summing over CZ areas, i.e., by applying $\Sigma_A \cdot$. Noting the cancellation of nucleation terms, one thus obtains

$$d/dt\, N_s = FA_{s-1}N_{s-1} - FA_s N_s \approx -Fd/ds(A_s N_s), \tag{9}$$

the familiar equations for the evolution of island densities for various sizes $s > 2$. Next, we apply $\Sigma_A A \cdot$ to (8). The analysis is more complicated here particularly because of the terms describing nucleation, for which we first require a more detailed characterization. The details of this analysis are presented in Appendix A, and lead to the following equation:

$$d/dt(A_s N_s) = F(A_{s-1})^2 N_{s-1} - F(A_s)^2 N_s$$
$$- A_{subnuc}(s)P_s d/dt\, N_{av} + \varepsilon_{s-1} - \varepsilon_s$$
$$\approx -Fd/ds[(A_s)^2 N_s] - A_{subnuc}(s)P_s d/dt\, N_{av}$$
$$- d/ds\, \varepsilon_s, \tag{10}$$

for $s > 2$, where $A_{subnuc}(s)$ denotes the average area of the portion or subset of the CZ of just nucleated islands which overlaps with CZs of islands of size s. This quantity satisfies (cf. Sec. IV)

$$A_{subnuc}(s)P_s = \Sigma_A A_{subnuc}(s,A)P_{s,A}, \quad \text{and}$$
$$\Sigma_s A_{subnuc}(s)P_s = A_{avsubnuc}M_0 = A_{avnuc}. \tag{11}$$

The "correction" terms[19] $\varepsilon_s = F\Sigma_A(A - A_s)^2 N_{s,A}$ give a measure of the variance of the CZ area distribution for islands of size s. The mathematical derivation of these terms is straightforward.[19] They simply reflect the general feature that the average of the product of quantities deviates from the product of the averages. These correction terms were ignored in our earliest formulation in Ref. 8 of rate equations for the A_s.

VI. SCALING ANALYSIS OF THE MOMENT EQUATIONS

One can of course directly analyze the equations (8)–(10) for any value of h/F. However, if the primary interest is in large s_{av}, then it is natural to attempt direct analysis of this regime by demonstrating that (8)–(10) support solutions with

a suitable scaling form (1). Indeed, this additional nontrivial step has already been performed in previous work[5,8–10] for simplified versions of the JPD equations, and certainly provides more insight into behavior of the solutions.

One can analyze the scaling form of the evolution equation (8) for the full JPD, as in Refs. 9 and 10. However, this analysis is rather complicated, and it is not necessary for our purposes. Instead, we focus on analysis of the reduced equations (9) and (10). We shall exploit the result that $s_{av} \sim \theta^z$, with $z = 2/3$ for point islands. Higher "effective" values of z (< 1) are found for compact islands for non-negligible θ, where nucleation is inhibited by finite island extent, but we claim that this does not reflect true scaling (cf. Sec. VIII). Following Refs. 5 and 9 and Appendix C, analysis of (9) yields the *fundamental equation for* $f(x)$:

$$(1 - 2z)f(x) - zx\, d/dx\, f(x) = -d/dx[a(x)f(x)]. \tag{12}$$

Indefinite integration of (12) provides an exact relation for

$$f(x) = f(0)\exp\left[\int_0^x dy\{(2z - 1) - a'(y)\}/\{a(y) - z\cdot y\}\right] \tag{13}$$

in terms of $a(x)$ and z.[5] Analysis of (10) requires adoption of the scaling forms (6) for the key quantities characterizing nucleation. Then, following the analysis in Appendix C, one obtains the *fundamental equation for* $a(x)$:

$$[a(x) - z\cdot x]d/dx\, a(x)$$
$$= (1 - z)\left[a(x) - f(x)^{-1}\int d\alpha\, a_{subnuc}(\alpha)q(\alpha)F(x,\alpha)\right]$$
$$- d/dx[v(x)f(x)]/f(x). \tag{14}$$

Definite integration over $[0, \infty]$ of (12) and (14), respectively, yields the constraints

$$a(0)f(0) = 1 - z$$

and

$$(1 - z)[a_{avsubnuc}M_0 - a(0)] = (1 - z)[a_{avnuc} - a(0)]$$
$$= v(0)f(0). \tag{15}$$

More precisely, the latter is most conveniently obtained by integration of the primitive form of Eq. (14) obtained directly from the derivation in Appendix C.

In the above equations $v(x) = \int d\alpha[\alpha - a(x)]^2 F(x,\alpha)$ denotes the variance of the scaled CZ area distribution, as already introduced in Sec. III. Previous studies reveal that $v(x)$ is small, and nearly independent of x.[9] Consequently, in the following analysis for point islands, we shall assume that $v(x) \approx v \approx 0.08$ (Ref. 9) is constant.

Using the factorization ansatz (2), i.e., $F(x,\alpha) = G[\alpha - a(x)]f(x)$, we can proceed to simplify the key equation (14) to obtain

$$[a(x) - z\cdot x]d/dx\, a(x)$$
$$= (1 - z)\left[a(x) - \int d\alpha\, a_{subnuc}(\alpha)q(\alpha)G(\alpha - a(x))\right]$$
$$- v[d/dx\, f(x)]/f(x). \tag{16}$$

Upon eliminating $f(x)$ from the last term of (16) using (12) (see Ref. 20), one obtains

$$d/dx\, a(x) = \frac{(1-z)\left[a(x) - \int d\alpha\, a_{\text{subnuc}}(\alpha)q(\alpha)G(\alpha-a(x))\right]\left[a(x)-z\cdot x\right]-(2z-1)v}{[a(x)-z\cdot x]^2-v},$$

$$(17)$$

which constitutes a closed equation for $a(x)$ upon assuming appropriate forms for $a_{\text{subnuc}}(\alpha)$, $q(\alpha)$, and G. (A Gaussian G suffices.) We will analyze this equation making the natural choice that $a_{\text{subnuc}}(\alpha) = \mu \cdot \alpha$, and that $q(\alpha) = c \cdot \alpha^{\text{neff}}$, with suitable n_{eff}. This leaves one parameter $\lambda = \mu \cdot c$, which may be chosen to satisfy the normalization conditions (7) mentioned above.

Finally, we comment on two aspects of the *mathematical structure* of Eq. (17). First, from simulation studies for point islands, it is known that $a(x) - z \cdot x$ decreases from a "large" initial value of $a(0) \approx 0.92$ for $x = 0$, to values for large x which are clearly below $v^{1/2} \approx 0.28$. Consequently, the denominator of (17) must vanish at some $x = x_s$ where $a_s = a(x_s) = z \cdot x_s + v^{1/2}$. At this point, the numerator and denominator must simultaneously vanish, so that the equation can be integrated through this removable singularity. Thus, by solving simultaneously the equations obtained from setting the numerator and denominator of (17) to zero, one can immediately determine the non-mean-field value of $a = a_s$ at $x = x_s$, and also see how it is controlled by the forms of a_{subnuc} and q. The nature of this singularity will be discussed further in Sec. VII, as well as the difficulties it generates in obtaining robust numerical solutions of (17).

Second, the above discussion raises the question: what is the asymptotic form of $a(x)$ versus x, for large x? From simulation results for point islands, it seems that $a(x)$ at least approaches close to $z \cdot x$, for large x. Equation (17) predicts that if $a(x) - z \cdot x \to 0$, then one has that $d/dx\, a(x) \to 2z - 1$. Thus, if $a(x)$ approaches $z \cdot x$, the feature that $a(x)$ must cross $z \cdot x$ follows from a comparison of slopes $2z - 1 < z$ (for $z < 1$). This result is particularly significant for the form of the island size distribution $f(x)$. Equation (13) indicates the possibility of a divergent singularity in $f(x)$ when the denominator of the integrand, $a(x) - z \cdot x$, vanishes. However, the above result from (17) shows that any such singularity would be removed by simultaneous vanishing of the numerator in (13). Furthermore, the finite value of the integrand in (13) when $a(x) = z \cdot x$ can be readily determined from (17).[22] A contrasting scenario is realized in mean-field treatments where $a(x)$ [which is not governed by (17)] increases slowly, so that $da/dx < 2z - 1$ when $a(x) = z \cdot x$, and $f(x)$ [which still satisfies (13)] exhibits a singularity at this crossing point.[5,21]

VII. RATE EQUATION PREDICTIONS OF $a(x)$ FOR POINT ISLANDS

We now examine the predictions of the rate equations in Sec. VI for $a(x)$ using $a_{\text{subnuc}}(\alpha) \approx \mu \cdot \alpha$, and using $q(\alpha) = c\,\alpha^{n_{\text{neff}}}$ with $n_{\text{eff}} \approx (4+\alpha)/(2+\alpha)$ to fit simulation data, and using a Gaussian G. Ideally (and ultimately) we will use the

evolution equation (17) to determine $a(x)$. However, the singular behavior of this equation described at the end of Sec. VI creates additional complications. Thus, to obtain an initial check on our theory while avoiding these complications, we instead use Eq. (16) where the last term on the right-hand side (RHS) is determined from simulation data for $f(x)$. We also use the initial condition $a(0) = 0.9$ also obtained from simulation data. The latter is consistent with the second relation in (15) between $a(0)$ and a_{avnuc}. Figure 4(c) shows that the result of integrating this equation recovers all the key features of $a(x)$ apparent in the simulation data of Fig. 4(a). These include both a plateau for $x < 1$, followed by a rapid increase for $x > 1$. Similar but somewhat less satisfactory results follow using the simpler form $q(\alpha) \propto \alpha^3$. However, the result of integrating (16) neglecting the last term, i.e., effectively setting the variance v to zero, shows much poorer agreement with the simulation data of Fig. 4(a). Taken together, these results support the validity of our evolution equations. They further demonstrate the importance of suitably describing nucleation through $q(\alpha)$, and even of incorporating "correction" terms in the evolution equation associated with the spread in CZ areas for each island size.

Next, we analyze the evolution equation (17). First, in Fig. 11, we show the sign behavior of the numerator and denominator of the RHS of (17) for various regions of the (a, x) plane. The numerator is positive (negative) below (above) the $\cap$-shaped curve, and vanishes along this curve. The denominator is positive (negative) above (below) the line $x = (a - v^{1/2})/z$, where $z = 2/3$, and vanishes along this line. The $\cap$-shaped curve and the line $x = (a - v^{1/2})/z$ cross at two
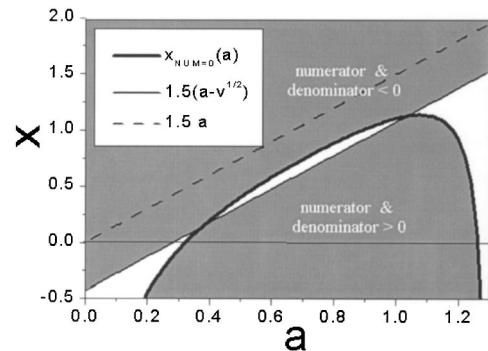

FIG. 11. Curves in the (a,x)-plane showing the zeroes of the numerator [$\cap$-shaped curve $x = x_{\text{NUM}=0}(a)$] and denominator [the line $x = (a - v^{1/2})/z$ or $a = z \cdot x + v^{1/2}$, where $z = 2/3$] of the RHS of Eq. (17). The right-most intersection of the $\cap$-shaped curve and this line at $x = x_s \approx 1.03$ and $a = a_s \approx 1.04$ is the "singular point" mentioned in the text. The line $x = a/z$ or $a = z \cdot x$ is also included for reference. The shaded area (not including its boundaries) gives the region where the RHS of (17) is positive, so $da/dx > 0$.

points, one of which is $a_s \approx 1.04$ and $x_s \approx 1.03$, using the notation of Sec. VI. Thus, the shaded region of the (a,x)-plane (excluding the boundaries) shows where the RHS of (17) is positive, and thus where $da/dx > 0$. The dashed line $x = a/z$ is also shown for reference. It is clear that the physical solution for $a(x)$ versus x, which starts at $a(0) \approx 0.9$ when $x=0$, must increase with increasing x to pass through the "singular point" (x_s, a_s), and can thereafter continue to increase further.

Finally, in Fig. 4(d), we show results of numerical integration of (17) for $a(x)$ versus x. Specifically, with our choice of initial conditions, $a(0) = 0.9$, one can numerically integrate (17) to a point close to (x_s, a_s) before singular behavior develops. We then step to a slightly large x value, and continue numerical integration to obtain the full curve shown. The solution crosses the line $z \cdot x$, where $z = 2/3$, with slope 1/3. The results reasonably match simulation data in Fig. 4(a), at least recovering the key qualitative features. However, we caution that the detailed behavior for larger x depends on exactly how one continues integration beyond the singular point, and unphysical behavior results from different choices than made here. These complications are not surprising since presumably one must have the exact initial condition and precise forms for $a_{subnuc}(\alpha)$ and $q(\alpha)$ in order to precisely recover the "exact" behavior of simulation data. Furthermore, in this analysis, we have largely ignored the fact that the VCs, which were used to determine $a_{subnuc}(\alpha)$ and $q(\alpha)$ in the simulations, do not correspond to the exact CZs.[5]

VIII. DISCUSSION

A primary contribution of this paper is the development and analysis of Eqs. (16) and (17). These equations show directly and unambiguously how the details of the nucleation process influence the form of $a(x)$ versus x, i.e., the variation of the CZ area A_s with island size s. This variation is of fundamental significance as it controls the shape of the island size distribution.[5] However, our treatment is not completely self-contained, requiring as input $a_{subnuc}(\alpha)$ and $q(\alpha)$, in addition to G and $a(0)$. Also, Eq. (17) has singular character, creating complications for robust numerical analysis with approximate input data. We might contrast this approach against MR[10] who use the more complicated equations for the full JPD, thus avoiding this singular behavior. However, their characterization of each nucleation event as fragmenting an existing CZ into two parts is not particularly realistic, although it suffices to recover solutions with qualitatively correct scaling behavior. Furthermore, in the light of our demonstration of the key role of nucleation in determining the evolution of CZ areas, one should question the approach of APF,[11,12] which ignores the effect of nucleation on existing CZ areas (other than applying a simple rescaling to maintain normalization). Despite its apparent success in predicting the island size dependence of capture numbers, this approach produces an unphysical delta-function scaling form for the JPD, and in some regimes produces unrealistic values for CZ areas.

Since all of the results and analysis of this paper have been for "idealized" point islands, it is appropriate to comment on any expected differences in behavior for nucleation and growth of compact islands. As noted previously, the latter occur in many real systems. Our perspective here is somewhat different from that of other groups. For compact islands in the scaling limit $h/F \to \infty$, we expect that true collapse of the island size distribution to a θ-independent scaling form actually occurs only in the low-θ point island regime, where the spatial extent of the islands is small. However, this scaling regime can run for many decades in θ from $\theta^* \sim (h/F)^{-1/2}$ to some $\theta \ll 1$ (say, 0.01 ML). Here, $s_{av} \sim \theta^z$ with $z = 2/3$, and the true scaling form will be described by the point island result. It is difficult for simulation studies to access behavior in this regime. Instead, simulations have focused on behavior at 0.1 ML or higher, a regime which likely does not exhibit any true scaling with θ. Effective values of z above 2/3 are typically found for compact islands since nucleation is inhibited relative to point islands, but it is not appropriate to identify $z = 1$ (corresponding to no nucleation) recalling that $f(0)a(0) = 1 - z > 0$.[9] Finite island extent for higher θ causes the size distribution to vary slightly with θ, coalescence of islands already occurring to some extent. Finite island extent also produces a modified quasilinear form of $a(x)$, especially for smaller h/F,[23] which does not follow from the scaling theories.[8–12] Undoubtedly, if one performs simulation studies for compact islands with smaller θ around 0.01 ML, say (which is well within the scaling regime, for large h/F), one would see more point-island-like behavior.

Finally, we note that previous simulation studies showed that island size distributions in models with point and compact islands were quite similar. However, simulations for models with fractal islands (created due to an absence of island restructuring following aggregation)[24] revealed sharper distributions *apparently* satisfying $f(0) = 0$. This has led to the common adoption for all models of postulated (but invalid) analytic forms for $f(x)$ with $f(0) = 0$.[25] We will provide a detailed discussion elsewhere of this "anomalous" behavior for fractal islands. However, we just note here that to most appropriately assess scaling, one should not consider behavior with increasing h/F for fixed θ (as done previously), but rather for a fixed effective coverage which measures the fractional area enclosed within the convex envelopes of the individual fractal islands.[26]

APPENDIX A: KEY QUANTITIES DESCRIBING SPATIAL ASPECTS OF NUCLEATION

Let $P_{s,A}(A_{subnuc})$ denote the probability that the CZ of a just-nucleated island overlaps an existing CZ of area A be-

longing to an island of size s by an amount A_{subnuc} (i.e., A_{subnuc} is the common overlap area). See Fig. 8(a). Then, one has that

$$P_{s,A} = \Sigma_{A\text{subnuc}} P_{s,A}(A_{\text{subnuc}}),$$

$$P_{s,A}^+ = \Sigma_{A\text{subnuc}} P_{s,A+A\text{subnuc}}(A_{\text{subnuc}}),$$

and   (A1)

$$A_{\text{subnuc}}(s,A) = \Sigma_{A\text{subnuc}} A_{\text{subnuc}} P_{s,A}(A_{\text{subnuc}})/P_{s,A}. \quad \text{(A2)}$$

From the first two relations in (A1), it is immediately clear that $\Sigma_A \cdot$ applied to $P_{s,A}$ and $P_{s,A}^+$ yields the same result, namely P_s. The primary task here is to elaborate on the moment analysis of the nucleation terms in (8) which leads to (10). Substituting in the above relations yields

$$\Sigma_A A(P_{s,A}^+ - P_{s,A}) = \Sigma_A \Sigma_{A\text{subnuc}} A P_{s,A} + A_{\text{subnuc}}(A_{\text{nuc}})$$
$$- \Sigma_A \Sigma_{A\text{subnuc}} [(A - A_{\text{subnuc}}) + A_{\text{subnuc}}]$$
$$\times P_{s,A}(A_{\text{subnuc}}). \quad \text{(A3)}$$

Making the change of variable $A = B + A_{\text{subnuc}}$ and replacing $\Sigma_A \cdot$ with $\Sigma_B \cdot$ in the first part of the second term shows that it cancels with the first term, thus yielding

$$\Sigma_A A(P_{s,A}^+ - P_{s,A}) = -\Sigma_A \Sigma_{A\text{subnuc}} A_{\text{subnuc}} P_{s,A}(A_{\text{subnuc}})$$
$$= -\Sigma_A A_{\text{subnuc}}(s,A) P_{s,A}$$
$$= -A_{\text{subnuc}}(s) P_s. \quad \text{(A4)}$$

Previous analysis by EB[9] and MR[10] assumed implicitly that

$$P_{s,A}(A_{\text{subnuc}}) = P_{s,A} \delta[A_{\text{subnuc}} - A_{\text{subnuc}}(s,A)], \quad \text{(A5)}$$

where δ is the delta function, i.e., Refs. 9 and 10 assume that the overlap area, A_{subnuc}, adopts a single value, $A_{\text{subnuc}}(s,A)$, rather than a distribution. In this approximation, one has[9]

$$P_{s,A}^+ = dA^+/dA \, P_{s,A+}, \quad \text{(A6)}$$

where A^+ satisfies $A^+ = A + A_{\text{subnuc}}(s,A^+)$. The first factor dA^+/dA appearing in $P_{s,A}^+$ comes from integrating over the above composite delta function. This is most clearly illustrated for the simple example $A_{\text{subnuc}}(s,A) = \mu A$, where

$$P_{s,A+A\text{subnuc}}(A_{\text{subnuc}})$$
$$= P_{s,A+A\text{subnuc}} \delta[A_{\text{subnuc}} - A_{\text{subnuc}}(s,A+A_{\text{subnuc}})]$$
$$= P_{s,A+A\text{subnuc}} \delta[(1-\mu)A_{\text{subnuc}} - \mu A]$$
$$= (1-\mu)^{-1} P_{s,A+A\text{subnuc}} \delta[A_{\text{subnuc}} - \mu(1-\mu)^{-1}A].$$
    (A7)

Then, using (A5) to calculate $P_{s,A}^+ = \Sigma_{A\text{subnuc}}$ $\times P_{s,A+A\text{subnuc}}(A_{\text{subnuc}})$ recovers (A6) noting the identities $A^+ = (1-\mu)^{-1}A$, and $dA^+/dA = (1-\mu)^{-1}$.[27] The key point is that this idealized choice (A5) does not change the outcome of the moment analysis producing equations (9) and (10) [or (A4)].

Our formulation of equations for evolution of the CZ areas involves only the area of the portion or subset, A_{subnuc}, of the CZ of just-nucleated islands overlapping with an existing CZ. However, it is natural to consider the total area, A_{nuc}, of the CZ of the just-nucleated island. See Fig. 8(a). Defining $A_{\text{nuc}}(\alpha) = A_{\text{av}} a_{\text{nuc}}(\alpha)$, the behavior of $a_{\text{nuc}}(\alpha)$ for just-nucleated islands with CZs overlapping CZs of existing islands with scaled area α is shown in Fig. 9(b). This quantity is more complicated than $a_{\text{subnuc}}(\alpha)$. The fact that the just-nucleated CZ overlaps an existing small CZ does not imply that its area is small, hence $a_{\text{nuc}}(\alpha)$ is not small when α is small. For comparison with the distribution of areas of CZs for islands with various fixed scaled sizes, in Fig. 5(a) we have shown the distribution of areas of CZs of just-nucleated islands. This distribution differs from the distribution of CZ areas for all dimers in Fig. 5(b) (as some of these CZ areas are impacted by subsequent nucleation events). This difference is reflected in the average values $A_2 \approx 0.92 A_{\text{av}}$ and $A_{\text{avnuc}} \approx 0.97 A_{\text{av}}$ for point islands. We have also noted that $A_{\text{avsubnuc}} = A_{\text{avnuc}}/M_0$ with $M_0 \approx 5.5$ for point islands.

APPENDIX B: DIFFUSION EQUATION ANALYSIS

We consider the rotationally invariant steady-state solution of the diffusion equation

$$\partial/\partial t N_1 = F + h\nabla^2 N_1 = F + hr^{-1}\partial/\partial r(r\partial/\partial r N_1) \approx 0, \quad \text{(B1)}$$

within the CZ of radius $r = r_{\text{CZ}}$ for an island radius $r = r_{\text{isl}}$ (both centered on the origin $r = 0$). Thus, one has the boundary conditions $N_1(r = r_{\text{isl}}) = 0$ and $\partial/\partial r N_1(r = r_{\text{CZ}}) = 0$. The solution is

$$N_1 = \frac{1}{2}(h/F)^{-1}(r_{\text{CZ}})^2 \ln(r/r_{\text{isl}})$$
$$+ \frac{1}{4}(h/F)^{-1}(r_{\text{isl}})^2[1 - (r/r_{\text{isl}})^2], \quad \text{(B2a)}$$

so that $\partial/\partial r N_1 = \frac{1}{2}(h/F)^{-1}r_{\text{CZ}}[(r_{\text{CZ}}/r) - (r/r_{\text{CZ}})].$
    (B2b)

The total nucleation rate within the CZ is given by

$$J = \int_{\text{CZ}} dr \, 2\pi r h(N_1)^2 = 2\pi h \frac{1}{2}(r_{\text{CZ}})^2[N_1(r = r_{\text{CZ}})]^2$$
$$+ 2\pi h \int_{\text{CZ}} dr(r^2 \partial/\partial r N_1)N_1 = \cdots, \quad \text{(B3)}$$

where the integrals range from $r = r_{\text{isl}}$ to $r = r_{\text{CZ}}$. Given the simple algebraic form of (B2b), it is easy to show from repeated integration-by-parts that J scales like $(r_{\text{CZ}})^6$ with logarithmic corrections.

APPENDIX C: DERIVATION OF THE SCALING FORM OFTHE MOMENT EQUATIONS

For completeness, we note that a scaling analysis of the various terms in (9) yields

$$d/dt\, N_s \approx F(s_{\mathrm{av}})^2[(1-2z)f - z \cdot x\, df/dx]$$

and

$$-F d/ds[A_s N_s] \approx -F(s_{\mathrm{av}})^2 d/dx(af), \qquad \text{(C1)}$$

from which one obtains (12), as in previous studies.[5,9] Of more central importance for this study is the observation that a similar analysis of the various terms in (10) is possible yielding

$$d/dt(A_s N_s) \approx -(t \cdot s_{\mathrm{av}})^{-1} z\, d/dx(xaf),$$

$$-F d/ds[(A_s)^2 N_s] \approx -(t \cdot s_{\mathrm{av}})^{-1} d/dx(a^2 f),$$

$$-\Sigma_A A_{\mathrm{subnuc}}(s,A)P_{s,A}\, d/dt\, N_{\mathrm{av}}$$

$$\approx -(1-z)(t \cdot s_{\mathrm{av}})^{-1} \int d\alpha\, a_{\mathrm{subnuc}}(\alpha)q(\alpha)F(x,\alpha),$$

$$\text{(C2)}$$

$$-d/ds\, \varepsilon_s \approx -(t \cdot s_{\mathrm{av}})^{-1} d/dx\left\{ \int d\alpha[\alpha - a(x)]^2 F(x,\alpha) \right\}.$$

Substituting these terms into (10), followed by some rearrangement utilizing (12), yields the key scaling equation (14) for $a(x)$.

---

[1] S. Stoyanov and D. Kashchiev, Curr. Top. Mater. Sci. **7**, 69 (1981); J. A. Venables, Philos. Mag. **27**, 693 (1973).

[2] M. C. Bartelt and J. W. Evans, Phys. Rev. B **46**, 12 675 (1992).

[3] G. S. Bales and D. C. Chrzan, Phys. Rev. B **50**, 6057 (1994).

[4] The mean-field treatment does account for spatial correlations in the island distribution, specifically the low population of near-by pairs of islands. This feature reflects the depleted adatom density, and thus nucleation rate, near island edges, which constitute sinks for diffusing adatoms.

[5] M. C. Bartelt and J. W. Evans, Phys. Rev. B **54**, R17359 (1996).

[6] J. A. Venables and D. J. Ball, Proc. R. Soc. London, Ser. A **322**, 331 (1971).

[7] P. A. Mulheran and J. A. Blackman, Phys. Rev. B **53**, 10 261 (1996) inappropriately equates island size and CZ area distributions, and proposes that no scaling with θ occurs for irreversible island formation.

[8] J. W. Evans and M. C. Bartelt, in *Morphological Organization in Epitaxial Growth and Removal*, edited by Z. Zhang and M. G. Lagally (World Scientific, Singapore, 1998), p. 50. Note the typographic error in the $a(x)$ equation. The general strategy of a rate equation approach for analyzing CZ areas was suggested by G. S. Bales at ACCG-10, 1996.

[9] J. W. Evans and M. C. Bartelt, Phys. Rev. B **63**, 235408 (2001).

[10] P. A. Mulheran and D. A. Robbie, Europhys. Lett. **49**, 617 (2000).

[11] J. G. Amar, M. N. Popescu, and F. Family, Phys. Rev. Lett. **14**, 3092 (2001).

[12] M. N. Popescu, J. G. Amar, and F. Family, Phys. Rev. B **64**, 205404 (2001).

[13] M. C. Bartelt, A. K. Schmid, J. W. Evans, and R. Q. Hwang, Phys. Rev. Lett. **81**, 1901 (1998); M. C. Bartelt, C. R. Stoldt, C. J. Jenks, P. A. Thiel, and J. W. Evans, Phys. Rev. B **59**, 3125 (1999).

[14] M. C. Bartelt and J. W. Evans, Surf. Sci. **298**, 421 (1993). See also K. J. Caspersen, A. R. Layson, C. R. Stoldt, V. Fournee, P. A. Thiel, and J. W. Evans, Phys. Rev. B **65**, 193407 (2002).

[15] APFs treatment yields $F(x,\alpha) = \delta(x-x(\alpha))g(\alpha) = f(x)\delta(\alpha - a(x))$. Here, $x(\alpha)$ is the inverse function of $a(x)$, and $g(\alpha) = x'(\alpha)f(x(\alpha))$ for $\alpha \geq a_{\min} = a(0)$, and $g(\alpha) \equiv 0$ for $\alpha < a(0)$.

[16] J. W. Evans, J. B. Hannon, M. C. Bartelt, and G. L. Kellogg, Bull. Am. Phys. Soc. **45**, 363 (2000).

[17] Implicitly, in our formulation, we assume that existing CZ boundaries are *not* modified outside the CZ of the just nucleated island. This is exactly true for VCs and ECs, and likely a good approximation for DCs.

[18] For notational simplicity, in this paper, we drop the * on these P's appearing in Ref. 9.

[19] Application of $\Sigma_A A \cdot$ to (8) yields terms of the form $\Sigma_A FA^2 \times N_{s,A} = \Sigma_A F[(A-A_s)^2 + 2A_s(A-A_s) + (A_s)^2]N_{s,A} = \varepsilon_s + F(A_s)^2 N_s$, thus generating "correction terms" ε_s.

[20] Equation (12) implies that $(df/dx)/f(x) = [(2z-1) - d/dx\, a(x)]/[a(x) - zx]$.

[21] Note that $f(x) \equiv 0$ for $x > x^*$, if $a(x^*) = z \cdot x^*$ and $d/dx\, a(x^*) > 2z - 1$ (Refs. 5 and 9).

[22] This value of the integrand is $(1-z)v^{-1}[a(x) - \int d\alpha\, a_{\mathrm{subnuc}}(\alpha)q(\alpha)G(\alpha - a(x))]$.

[23] F. G. Gibou, C. Ratsch, M. F. Gyure, S. Chen, and R. E. Caflisch, Phys. Rev. B **63**, 11 505 (2001). See C. Ratsch, M. F. Gyure, S. Chen, M. Kang, and D. D. Vvedensky, *ibid.* **61**, R10 598 (2000); D. D. Vvedensky, *ibid.* **62**, 15 435 (2000) for other relevant work of this group.

[24] L. H. Tang, J. Phys. (Paris) **3**, 935 (1993).

[25] J. G. Amar and F. Family, Phys. Rev. Lett. **74**, 2066 (1995); H. Brune, Surf. Sci. Rep. **31**, 121 (1998).

[26] M. C. Bartelt and J. W. Evans, Surf. Sci. Lett. **314**, L835 (1994).

[27] In physical terms, islands of size s with CZ area A are created when CZs of just-nucleated islands overlap CZs of existing islands of size s with larger area of $A^+ = (1-\mu)^{-1}A$. Suppose $\mu = 1/2$, so $A^+ = 2A$. The factor of $dA^+/dA = 2$ is needed in $P_{s,A}^+$ since there are typically two initial (discrete) CZ areas A^+ which will produce a final (discrete) CZ area A.